



# Forces acting on the clavicle during shoulder abduction, forward humeral flexion and activities of daily living

P. Hoogervorst<sup>a,\*</sup>, B. Bolsterlee<sup>b,c,1</sup>, M. Pijper<sup>d</sup>, A. Aalsma<sup>d</sup>, N. Verdonshot<sup>a,e</sup>

<sup>a</sup> Department of Orthopedics, Radboud University Medical Center, Nijmegen, the Netherlands

<sup>b</sup> Neuroscience Research Australia (NeuRA), Sydney, New South Wales, Australia

<sup>c</sup> Graduate School of Biomedical Engineering, University of New South Wales, Sydney, New South Wales, Australia

<sup>d</sup> BAAT Medical BV, Hengelo, the Netherlands

<sup>e</sup> Department of Biomechanical Engineering, University of Twente, Enschede, the Netherlands

## ARTICLE INFO

### Keywords:

Clavicle  
Forces  
Biomechanics  
Simulation  
Delt Shoulder and Elbow Model

## ABSTRACT

**Background:** The forces acting on the human clavicle in vivo are difficult if not impossible to measure. The goal of this study is to quantify the forces acting on the human clavicle during shoulder abduction, forward humeral elevation and three activities of daily living using the Delt Shoulder and Elbow Model.

**Methods:** The Delt Shoulder and Elbow Model and a computed tomography scan of a clavicle were used to calculate the forces and moments acting on the entire clavicle and on three planes within the middle third of the clavicle during the simulated movements.

**Findings:** The largest resultant force simulated across the clavicle was 126 N during abduction. Maximum resultant moments of 2.4 Nm were identified during both abduction and forward humeral elevation. The highest forces in the middle third of the clavicle were of a compressive nature along the longitudinal axis of the clavicle, increasing to 97 N during forward humeral elevation and 91 N during abduction. Forces in opposite direction along the y-axis were identified on either side of the conoid ligament. The three simulated activities of daily living had similar ranges of forces and moments irrespective of the sagittal plane in which these activities were performed.

**Interpretation:** Peak forces occurred at different locations on the middle third of the clavicle during different movements. The results create an understanding of the forces and their distribution across the clavicle during activities of daily living. These data may be helpful in the development of clavicular fixation devices.

**Level of evidence:** Biomechanical study.

## 1. Introduction

Clavicle fractures are common, comprising 5–10% of all fractures in adults (Robinson, 1998). Though classically managed non-operatively, clavicle fractures are now increasingly treated surgically (Huttunen et al., 2016). This is probably because of better short-term functional results, cosmetic satisfaction, earlier return to sports and cost effectiveness compared to non-operative treatments (Althausen et al., 2013; Kong et al., 2014; McKee et al., 2012; Robertson et al., 2018; Zlowodzki et al., 2005). The rise in surgical interventions has resulted in a plethora of different plate types, configurations and intramedullary devices to surgically reduce and fixate these fractures. These devices have been evaluated biomechanically. Load to failure testing of different fixation techniques (Chen et al., 2016; Demirhan et al., 2011; Drosdowech et al.,

2011; Little et al., 2012; Renfree et al., 2010; Toogood et al., 2014; Uzer et al., 2017) are reported to range from 100 to 409 N. (Demirhan et al., 2011; Little et al., 2012; Renfree et al., 2010; Uzer et al., 2017). Bio-mechanical studies typically conclude that “more and larger metal is stronger” though more metal may not necessarily be the best clinical option (Hulsmans et al., 2018; Mellema et al., 2014).

Optimal design of clavicle fixation devices requires knowledge of the forces that act on the clavicle during shoulder movements and activities of daily living. However, it remains unclear which loading thresholds fixation constructs have to withstand (Hulsmans et al., 2018), because these forces are difficult if not impossible to measure directly in vivo.

Cadaver testing has provided some insights into the forces acting on the clavicle. One study measured forces directly on a cadaveric clavicle

\* Department of Orthopedics, Radboud University Medical Center, P.O. Box 9101, 6500 HB Nijmegen, the Netherlands

E-mail address: [paul.hoogervorst@radboudumc.nl](mailto:paul.hoogervorst@radboudumc.nl) (P. Hoogervorst).

<sup>1</sup> Shared first authorship: Both authors have contributed equally to the development of this manuscript.

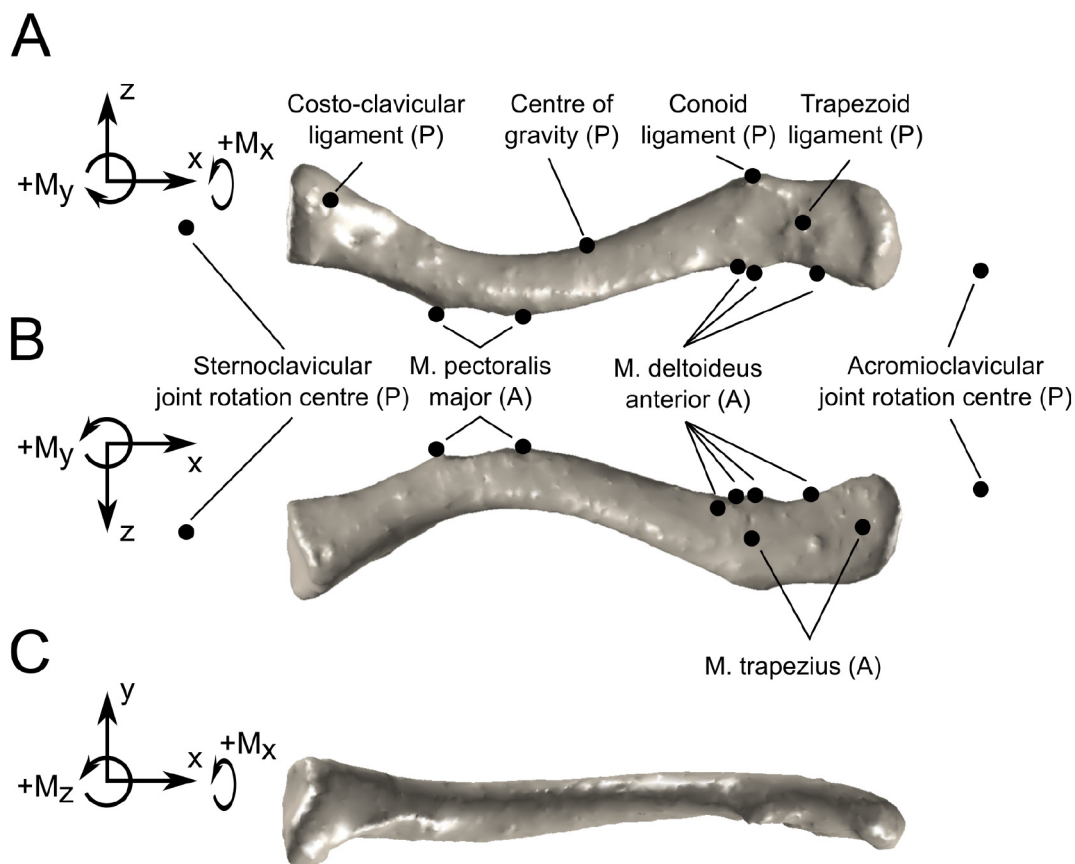


Fig. 1. Three-dimensional model made from a CT scan showing the 14 points of application of the forces acting on the clavicle as simulated with the DSEM. A = Inferior View, B Superior View, C Anterior View. P = passive forces, A = Active forces.

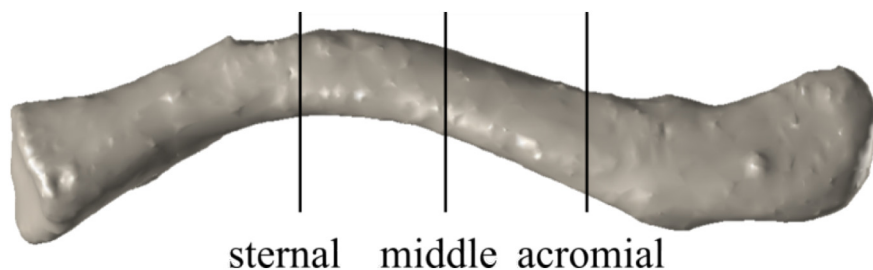


Fig. 2. Superior view of the clavicle, showing the three planes of interest on the sternal side, the middle and the acromial side of the middle third of the clavicle.

during shoulder movements using a six degree-of-freedom load cell (Iannolo et al., 2010). Limitations of this study were that the static forces used to stabilize the shoulder before starting a dynamic motion were variably selected and some major muscle groups were not included. Furthermore, only the forces during abduction and internal and external rotation were measured, omitting those during forward humeral elevation or more complex motions used during daily living activities.

Another way to quantify forces acting on the clavicle is by using a biomechanical computer model. Because the clavicle is part of the closed kinematic chain that also comprises the scapula and thorax, a comprehensive description of the shoulder girdle is required to get a realistic estimate of the forces acting on the clavicle. The Delft Shoulder and Elbow Model (DSEM) is a comprehensive musculoskeletal model of the human shoulder and elbow that includes all large bones and muscles of the upper limb (Bolsterlee et al., 2014; Nikooyan et al., 2011; van der Helm, 1994a; van der Helm, 1994b). The DSEM has been verified qualitatively by comparing predicted muscle forces to measured EMG signals and validated quantitatively by comparing predicted

glenohumeral (GH) joint contact forces to direct measurements made with an instrumented shoulder prosthesis (Nikooyan et al., 2010; Nikooyan et al., 2012). The DSEM is amongst the most detailed and well-validated models of the human upper limb to date.

The goal of this study is to quantify the forces acting on the human clavicle during shoulder abduction, forward humeral elevation and three activities of daily living (washing axilla, eating and combing hair). The DSEM was used to simulate the mechanical behavior and loading of all major muscles and bones of the shoulder and to generate data that may be helpful in the development of future clavicular fixation devices.

## 2. Methods

Since anonymized and publicly available data were used, this study was exempt from approval by an institutional review board. We used the DSEM (version 4–2) and a computed tomography (CT) scan of the same clavicle as used to develop the DSEM (Klein Breteler et al., 1999a) to calculate the forces acting on the clavicle during shoulder abduction

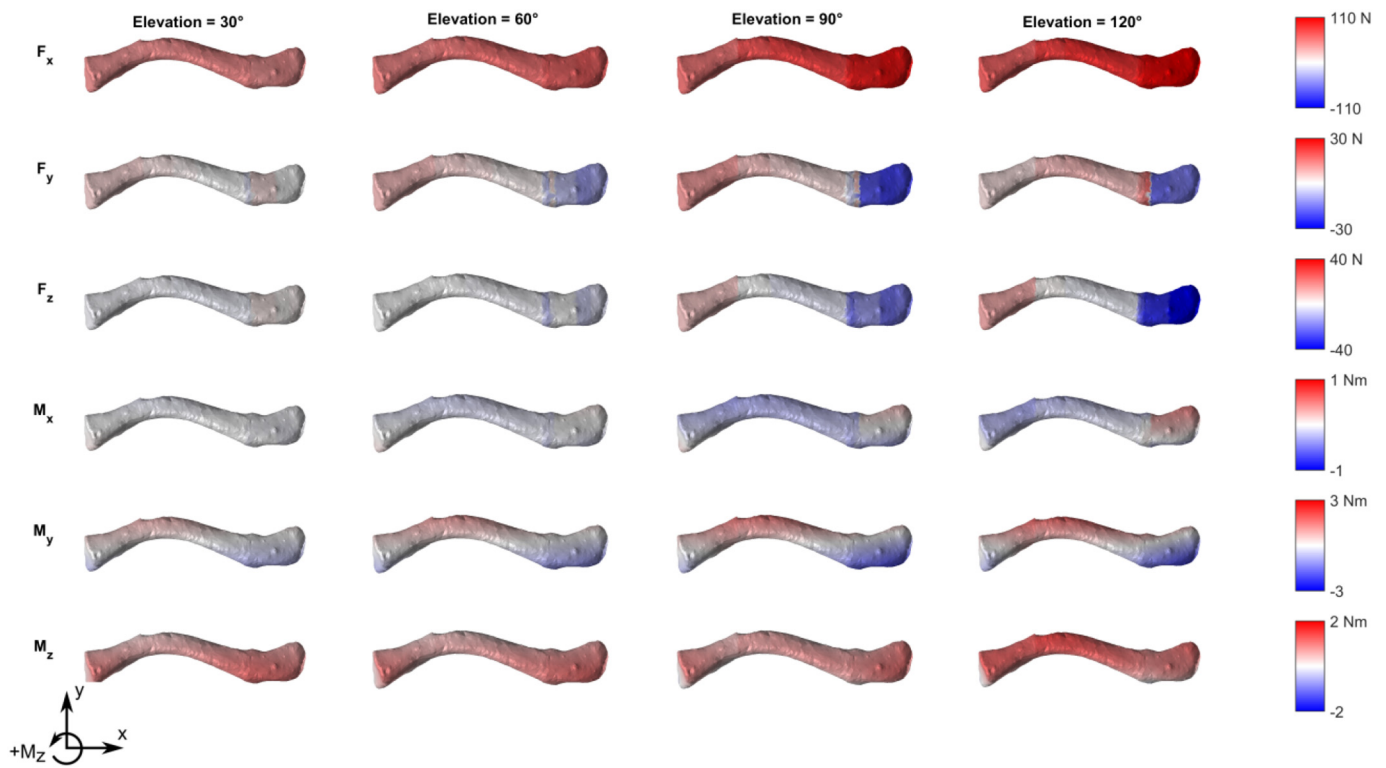


Fig. 3. Superior view of the clavicle and the estimated forces and moments at 30° intervals of shoulder forward humeral elevation (increasing elevation from left to right). Forces (top three rows) and moments (bottom three rows) acting on the clavicle in all three orthogonal directions are represented as colours projected on the muscle surface. Note that forces and moments in different directions have different colour scales (see colour bars on the right). (For interpretation of the references to colour in this figure legend, the reader is referred to the web version of this article.)

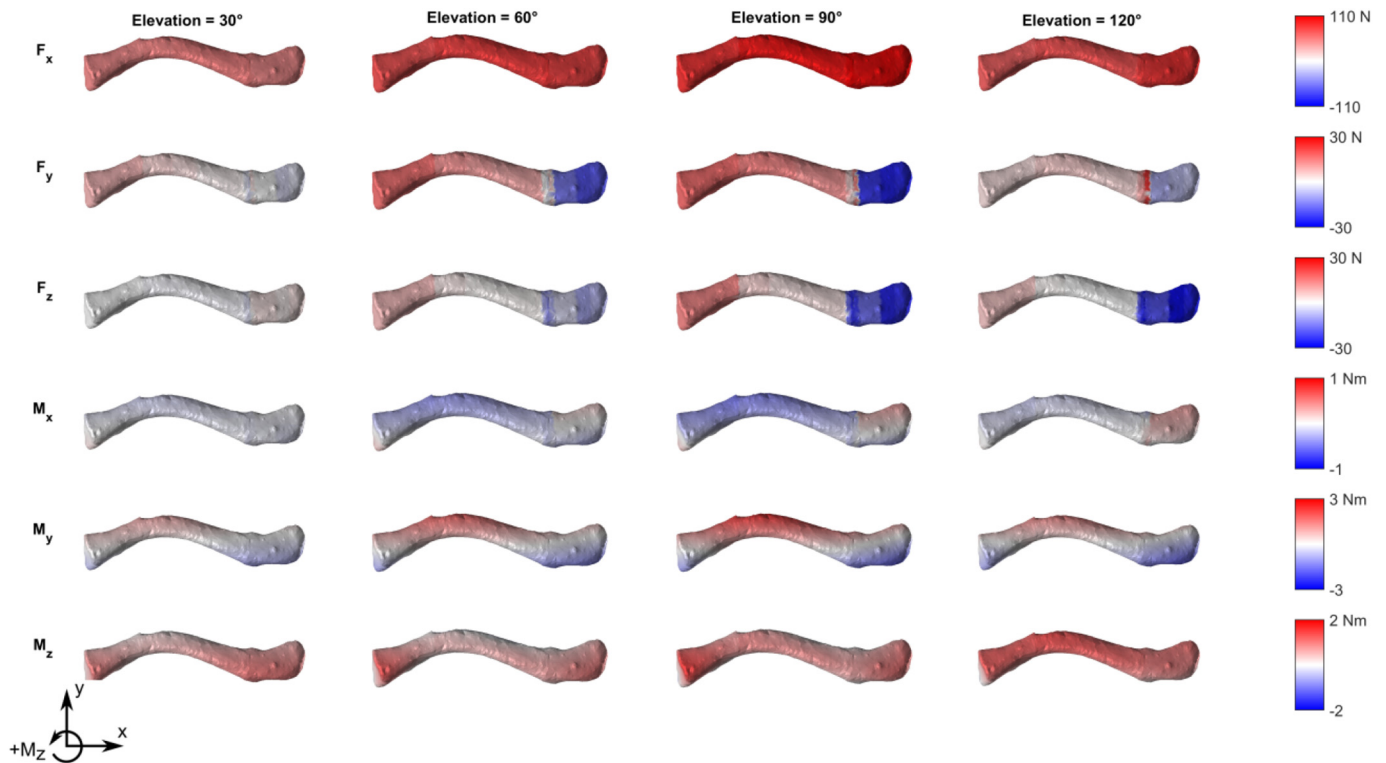


Fig. 4. Superior view of the clavicle and the estimated forces and moments at 30° intervals of shoulder abduction (increasing elevation from left to right). Forces (top three rows) and moments (bottom three rows) acting on the clavicle in all three orthogonal directions are represented as colours projected on the muscle surface. Note that forces and moments in different directions have different colour scales (see colour bars on the right). (For interpretation of the references to colour in this figure legend, the reader is referred to the web version of this article.)

**Table 1**

Minimum and maximum forces and moments within the middle third of the clavicle at the three (sternal, middle, lateral) planes for all five simulated movements. The numbers in parentheses represent the maximum forces simulated across the entire clavicle. Bold numbers represent the maximum simulated forces and moments.

Axis	Minimum force (N)	Maximum force (N)	Minimum moment (Nm)	Maximum moment (Nm)
<b>Abduction</b>				
X	37.5 (34.2)	90.9 (118.2)	-0.3 (-0.5)	0 (0.4)
Y	-0.8 (-21.8)	8.0 (19.0)	-0.9 (-1.4)	1.9 (2.0)
Z	-5.3 (-40.3)	13.3 (13.3)	-0.4 (-0.9)	1.2 (1.3)
Resultant		91.3 (126.1)		2.1 (2.4)
<b>Forward humeral elevation</b>				
X	29.4 (29.4)	96.5 (105.2)	-0.4 (-0.5)	0.1 (0.4)
Y	-0.9 (-25.9)	13.8 (22.8)	-0.5 (-1.0)	2.2 (3.2)
Z	-2.8 (-34.5)	4.3 (13.4)	-0.7 (-0.8)	1.2 (1.4)
Resultant		97.3 (111.3)		2.2 (2.4)
<b>Wash axilla</b>				
X	27.3 (27.2)	64.2 (64.2)	-0.4 (-0.5)	0.0 (0.3)
Y	-4.6 (-25.9)	9.7 (20.3)	-1.3 (-0.9)	1.5 (1.9)
Z	-5.7 (-8.7)	0.4 (8.7)	-1.2 (-2.2)	1.4 (1.1)
Resultant		64.5 (64.5)		1.6 (1.8)
<b>Eat</b>				
X	26.2 (26.0)	57.1 (60.3)	-0.3 (-0.4)	0.0 (0.2)
Y	-2.6 (-25.2)	13.8 (15.2)	-0.4 (-1.1)	1.2 (1.3)
Z	-2.5 (-16.2)	5.1 (15.7)	-0.9 (-1.0)	0.9 (1.2)
Resultant		55.4 (65.8)		1.4 (1.5)
<b>Comb hair</b>				
X	27.6 (27.4)	65.1 (80.0)	-0.3 (-0.4)	0.0 (0.3)
Y	-0.1 (-26.1)	10.6 (11.7)	-0.3 (-1.4)	1.5 (1.5)
Z	-0.9 (-25.9)	8.5 (10.4)	-0.6 (-0.8)	1.0 (1.2)
Resultant		51.2 (84.7)		1.6 (1.6)

and forward humeral elevation, as well as three motions used in daily living activities in which the humerus moves in different planes (washing axilla, eating and combing hair).

## 2.1. Quantification of clavicular loading with the Delft Shoulder and Elbow Model

The DSEM (Nikooyan et al., 2011; van der Helm, 1994b) was used in the inverse dynamic mode to estimate the forces acting on all shoulder muscles, joints and ligaments. Three-dimensional kinematic data of the forearm, humerus, scapula, clavicle and thorax were obtained from the publicly available Shoulder Movements Database (Bolsterlee et al., 2014). The kinematic data were used as input to calculate joint torques around the shoulder and elbow joints for each step of the movement. Static optimization with a minimal energy expenditure criterion was used to estimate a set of muscle forces that resulted in the joint torques (Praagman et al., 2006).

All forces acting on the clavicle were extracted from the model predictions. In total, the DSEM predicts 14 force vectors (point loads) on the clavicle (Fig. 1), which include the sternoclavicular (SC) and acromioclavicular (AC) joint contact forces; the gravitational and inertial forces of the clavicle; the forces on the conoid, trapezoid and costo-clavicular ligaments; and the forces of the pectoralis major, deltoid (clavicular/anterior part) and trapezius (clavicular part) muscles.

To accurately simulate the mechanical behavior of muscles with broad attachments, the DSEM represents the clavicular parts of the pectoralis major, trapezius and deltoid with two, two and four force vectors, respectively (Van der Helm and Veenbaas, 1991). The magnitude, direction and point of application was calculated for each of the 14 forces, and for each step of the movement. All forces were represented in a local clavicle-based coordinate system which was defined according to the convention of the International Society of Biomechanics (Wu et al., 2005). The x-axis is parallel to the line connecting

the sternoclavicular (SC) and acromioclavicular (AC) joint centers, the z-axis is perpendicular to the x-axis and the inferior-superior axis of the thorax (because only two bony landmarks can be discerned on the clavicle), and the y-axis is perpendicular to the x- and z-axes.

## 2.2. Estimation of loads on the clavicular surface

We calculated the maximum forces and moments on the clavicle, and the locations within the middle third of the clavicle where these maxima occurred. To estimate the (static) forces and moments acting on the clavicle, a three-dimensional (3D) clavicle surface model was created from a CT scan of the same clavicle used in the DSEM (male, 57 years, right-side) (Klein Breteler et al., 1999b). After outlining the clavicle on the CT scan using a combination of intensity thresholding and manual correction, a 3D triangulated surface mesh of the clavicular surface was created using image processing software 3D Slicer (Fedorov et al., 2012). The CT-based clavicle model was presented in a different coordinate system than the clavicle in the DSEM, so these coordinate systems were aligned. Prior to CT scanning and cadaver measurements (in which muscle and ligament attachment sites were defined (Klein Breteler et al., 1999b), four screws were drilled into the clavicle. The locations of the screw heads, which were clearly visible on the CT scan, were digitized during the cadaver measurements and were now also (virtually) digitized on the CT scan. The optimal rigid-body rotation was found between the screw head locations from CT and cadaver measurements. After alignment, the residual error between the four screw head locations ranged from 0.3 to 0.8 mm, indicating excellent alignment.

Static forces and moments at all points on the clavicular surface (i.e. all nodes of the surface mesh) were calculated using static equilibrium theory ("freebody diagram method"). For a given point on the clavicle (point P), the clavicle was (virtually) cut in the yz plane (plane perpendicular to the clavicle's long axis) at the x-value of P. To calculate the forces at P, all forces on one side of the cut-plane were summed. To calculate the moments at P, all forces on one side of the cut-plane were multiplied by their moment arm vector around P (the position vectors connecting point P and the point of application of the force) and then summed. Forces in the x-direction were interpreted as compression of the clavicle in the direction of its long axis. Forces in the y- and z-direction were interpreted as shear forces in the plane perpendicular to the clavicle's long axis. Moments around the x-axis were interpreted as torsion while moments around the y- and z-axis were interpreted as bending moments. Furthermore, resultant forces and moments were calculated for all simulated movements.

A focused analysis on the forces and moments in three planes within in the middle third of the clavicle was performed (Fig. 2), since these are the locations where about 80% of clavicle fractures occur and where the clavicle fixation devices are placed (Robinson, 1998). The three planes were located perpendicular to the clavicle's long axis (yz-plane) on the sternal (medial) and acromial (lateral) side of the middle third of the clavicle, and in the middle of the clavicle (Fig. 2).

## 3. Results

The estimated forces and moments on the clavicular surface were graphically represented at 30° intervals of shoulder abduction (Fig. 3) and forward humeral elevation (Fig. 4). The highest forces identified across the clavicle during abduction were of a compressive nature along the x-axis, increasing to 118 N. These compressive forces on the clavicle were predominantly generated by the sternoclavicular and acromioclavicular joint reaction forces (Supplementary Material 1). Within the middle third of the clavicle the maximum forces along the x-axis were simulated at 91 N. The maximum resultant force on the entire clavicle was estimated at 126 N during abduction (Table 1). The largest moment on the entire clavicle was 2.0 Nm around the y-axis during abduction. The maximum resultant moment during abduction was calculated at

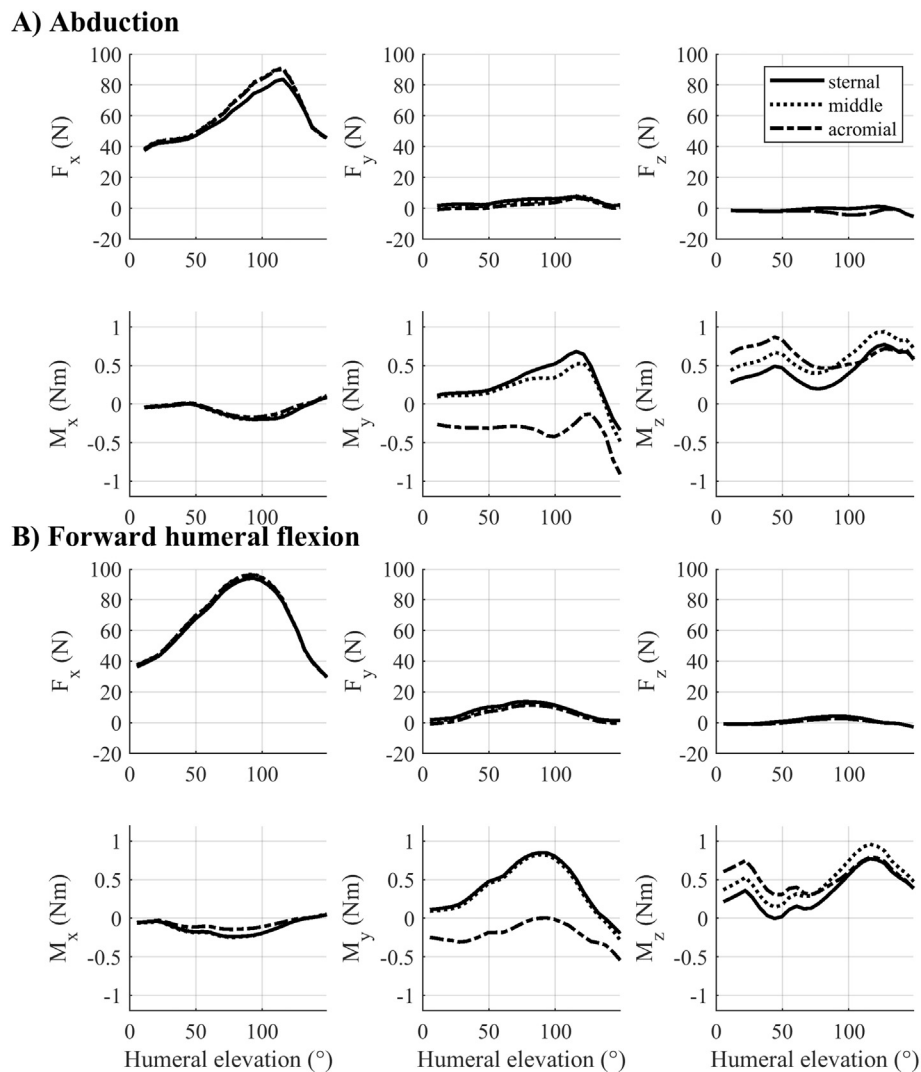


**Fig. 5.** Forces (top row) and moments (bottom row) acting on the clavicle at the planes of interest as a function of humeral elevation for (A) abduction and (B) forward humeral flexion. Traces are shown for forces and moments acting on the sternal (solid line), middle (dotted line) and acromial (dash-dotted line) side of the middle third of the clavicle.

2.4 Nm.

Shear forces were calculated along the y-axis at the lateral end of the clavicle, at the origin of the conoid ligament. Medial of the conoid ligament the forces along the y-axis were oriented in a positive direction, while lateral of the conoid ligament the forces were directed in a negative direction. These shear forces were simulated at 30, 60, 90 and 120° of shoulder abduction which were 2.7 N, 18.5 N, 34.3 N, 32.0 N. The maximum shear force was calculated at 37 N at 100° during abduction.

Similar to the abduction movement, the maximum resultant forces and moments acting on the entire clavicle during forward humeral flexion were calculated to increase to 111 N and 2.4 Nm at 90°. During this movement, the largest forces were simulated along the x-axis at 105 N. Within the middle third of the clavicle the maximum forces along the x-axis were simulated at 97 N. Force vectors along the y-axis in opposing directions (shear forces) were identified at the lateral side of the clavicle on either side of the conoid ligament. These maximum shear forces were calculated at 34 N along the y-axis at 116° of forward humeral flexion. At 30, 60, 90 and 120° of forward humeral flexion these forces were 0 N, 9.1 N, 24.9 N, 31.0 N.

When evaluating the forces and moments acting on the middle third of the clavicle, the maximum resultant force and moment occurred during forward humeral flexion and were 97 N and 2.2 Nm, respectively

(Table 1). All forces and moments at the middle third of the clavicle when the arm was elevated above 90° remained equal or decreased except for the moments around the z-axis during both abduction and forward humeral elevation. The minimum and maximum forces and moments across the entire clavicle and within the middle third of the clavicle for all five simulated movements are shown in Table 1.

Fig. 5 shows that the magnitude of forces and moments at the sternal, middle and acromial planes within the middle third of the clavicle were similar during abduction and forward humeral elevation, though distributed differently. The maximum forces were calculated along the x-axis at the middle and acromial planes while the minimum forces were calculated at the sternal plane.

When evaluating the three activities of daily living (washing axilla, eating, combing hair) a similar range of forces and moments was identified irrespective of the sagittal plane in which these activities were performed. The simulated moments around the x-axis were similar during all three movements. The maximum positive moments around the y-axis occurred at the sternal plane while the maximal negative moments around the y-axis occurred at the acromial plane. The maximal positive moments around the z-axis occurred at the acromial side while the maximal negative moments around the z-axis occurred at the sternal plane (Fig. 6).

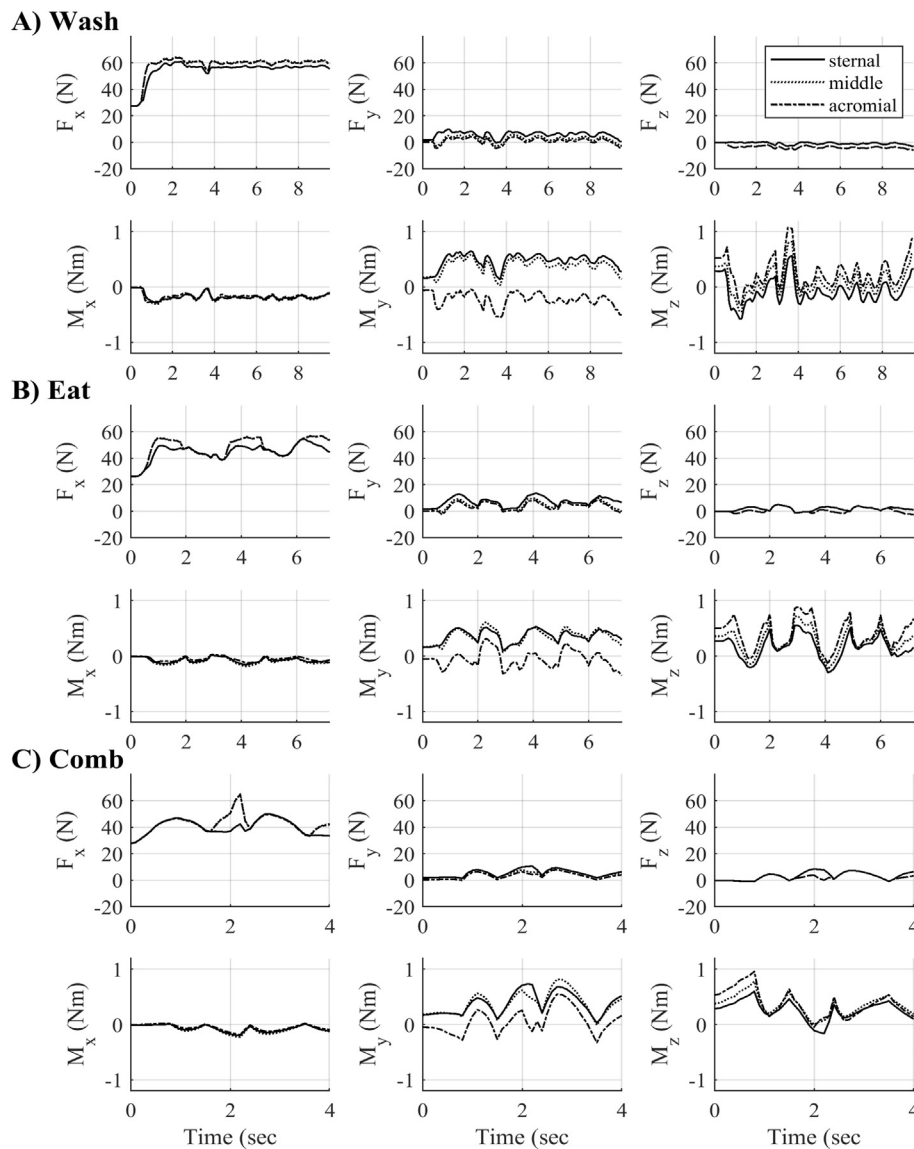


**Fig. 6.** Forces (top row) and moments (bottom row) acting on the clavicle at the planes of interest as a function of time during (A) Washing axilla (B) Eating and (C) Combing hair. Traces are shown for forces and moments acting on the sternal (solid line), middle (dotted line) and acromial (dash-dotted line) side of the middle third of the clavicle.

#### 4. Discussion

The goal of this study was to simulate the forces acting on the human clavicle using the DSEM in abduction, forward humeral elevation and three activities of daily living in order to better understand their magnitude and behavior.

We identified maximum compressive forces along the x-axis of 97 N during abduction and 91 N during forward humeral elevation in the middle third of the clavicle. No tensile forces along the x-axis were calculated during these motions signifying a continuous compressive force. The maximum resultant forces were larger outside of the middle third of the clavicle (126 N and 111 N, respectively). All of the maximum moments occurred outside the middle third. The minimum forces around the y-axis showed the largest discrepancy between forces measured in the middle third and the rest of the clavicle. These minimum forces most likely occur at the lateral end of the clavicle distal to the conoid ligament.

Comparing our outcomes to the results reported by Iannolo et al. (2016) could only be done for the abduction movement. Their group also identified that compressive forces were dominant with a maximum

value of 34.4 N (SD 22.3) during at 79.8° (SD 18.6) of abduction. Furthermore, a maximum tensile load of -5.2 N (SD 8.0) was found. Our findings for 90° of humeral abduction yielded a maximum compressive force almost 3 times higher and showed no tensile loading along the x-axis. Part of this difference may be explained by the different methods used to estimate the forces (experimental vs simulation). Additionally, Iannolo et al. established a static balance situation by applying weights to the shoulder cuff muscles and ligaments and used this as a zero-reference before starting the dynamic movement measurements. Therefore, it is to be expected that our findings yield higher results.

Comparing the peak torsion; Iannolo et al. measured the torsion around the x-axis to be 0.4 Nm, whereas we calculated a force around the x-axis during abduction of 0.1 Nm. Other than observe the fact that these results seem similar and seem to confirm the validity of the DSEM, no definitive conclusions can be drawn. Moments around the y-axis were found to be the largest in all simulated movements especially during abduction and forward humeral elevation indicating that bending moments perpendicular to the longitudinal axis in a grossly superior-inferior direction were dominant. This reflects a probable clinical mechanism for failure of fixation devices and serves as another

verification of the simulation generated by the DSEM.

Interestingly we identified that rotational forces around the longitudinal axis of the clavicle were the smallest which, theoretically, is to be expected due to the short lever arm but is feared by clinicians since this is thought to be one of the reasons for failure of plate fixation.

A decrease in forces across the clavicle was simulated during abduction and forward humeral elevation in the 90–120° interval. Most physical therapy (PT) protocols initially limit motion above 90° of abduction/forward humeral elevation. This finding raises questions about the necessity of this restriction. However, the moments around the z-axis continue to increase in this interval. Furthermore, GH-joint contact forces and thus possibly the forces across the clavicle estimated by the DSEM are well validated for movements up to 90° of humeral elevation, but for movements above the shoulder line the model underpredicted the measured force by, on average, 31%. (Nikooyan et al., 2010; Nikooyan et al., 2012) Further research on the forces and moments above 90° of abduction and elevation to evaluate possible implications for rehabilitation protocols needs to be initiated.

Evaluating the forces on the middle section of the clavicle during washing the axilla, combing hair and eating, comparable forces and moments were simulated in all three planes with a maximum of 65 N and 1.6 Nm. All forces were lower than those during isolated abduction and forward humeral elevation. Minimum and maximum forces and moments occur at different locations during different movements; this is important to realize when developing future clavicular fixation devices.

Another interesting finding is that the simulations showed that forces act in opposing directions along the y-axis on either side of the conoid ligament at the acromial end of the clavicle. Due to the muscle insertions medial of the conoid ligament and the weight of the arm on the lateral side, this may not be a surprising finding in itself. However, to the authors' knowledge this is the first study to quantify these forces at this location. Failure of fixation in lateral clavicle fractures is a known complication and is attributed to lack of cortical surface for screw placement and cranially directed forces of the medial end. The findings of the DSEM simulations may contribute to a better understanding of the failure of fixation.

One of the limitations of this study includes the validity of the predictions of the DSEM, and the assumptions made during the calculations. The forces acting on the clavicle may have been underestimated by the inability to account for muscle co-contraction using the inverse dynamic modelling approach used here, and by not including the external forces which are exerted on the hand during the ADL tasks (e.g. the hand pushing into the axilla for washing). These introduce an unknown margin of error in the results; however currently it is one of the best simulation models available and the outcomes seem comparable and realistic with direct measurements on physical models. Another limitation is that we did not simulate internal and external rotations. We do not expect the exclusion of these movements to have influenced the main findings significantly, since the majority of the forces during rotation will act at the level of the glenohumeral joint and not the clavicle itself. The fact that the DSEM is originally a shoulder-oriented model is the cause of the third limitation being that the sternocleidomastoid muscle was not included in the simulation which could influence the results. A fourth limitation is that we only evaluated the forces and moments across the clavicle in a non-weightbearing state. It is of interest to conduct further research on if and how weightbearing would influence the results. However, the forces and moments on the clavicle are clinically most relevant in the early stages of rehabilitation after surgical treatment of midshaft clavicle fractures, as rehabilitation generally consists of rest, and passive range of motion exercises for several weeks followed by non-weight bearing active range of motion exercises until fracture union has occurred. This initial timeframe is of particular interest because the forces that occur in this phase could lead to loss of fixation or hardware failure. Once united, the osseous parts of the clavicle, and not the fixation device, will bear most of the load. One

of the strengths of this study is that it is the first to simulate and quantify the forces and moments across the clavicle during forward humeral elevation and activities of daily living. Another strength is the inclusion of all but one of the muscle groups and ligaments involved in the motion of the clavicle.

## 5. Conclusion

The largest resultant force and moment simulated across the clavicle was 126 N during abduction and 2.4 Nm during both forward humeral elevation and abduction, respectively. Minimum and maximum forces occurred at different locations on the middle third of the clavicle during different movements. The results create an understanding of the forces across the clavicle during shoulder abduction, forward humeral elevation and activities of daily living.

Supplementary data to this article can be found online at <https://doi.org/10.1016/j.clinbiomech.2019.07.001>.

## Declaration of Competing Interest

There are no conflicts of interests for any of the authors.

## References

- Althausen, P.L., Shannon, S., Lu, M., O'Mara, T.J., Bray, T.J., 2013. Clinical and financial comparison of operative and nonoperative treatment of displaced clavicle fractures. *J Shoulder Elbow Surg* 22, 608–611. <https://doi.org/10.1016/j.jse.2012.06.006>.
- Bolsterlee, B., Veeger, H.E., van der Helm, F.C., 2014. Modelling clavicular and scapular kinematics: from measurement to simulation. *Med Biol Eng Comput* 52, 283–291. <https://doi.org/10.1007/s11517-013-1065-2>.
- Chen, Y., Yang, Y., Ma, X., Xu, W., Ma, J., Zhu, S., et al., 2016. A biomechanical comparison of four different fixation methods for midshaft clavicle fractures. *Proc Inst Mech Eng H* 230, 13–19. <https://doi.org/10.1177/0954411915611159>.
- Demirhan, M., Bilsel, K., Atalar, A.C., Bozdag, E., Sunbuloglu, E., Kale, A., 2011. Biomechanical comparison of fixation techniques in midshaft clavicular fractures. *J Orthop Trauma* 25, 272–278. <https://doi.org/10.1097/BOT.0b013e3181ee3db7>.
- Drosdowech, D.S., Manwell, S.E., Ferreira, L.M., Goel, D.P., Faber, K.J., Johnson, J.A., 2011. Biomechanical analysis of fixation of middle third fractures of the clavicle. *J Orthop Trauma* 25, 39–43. <https://doi.org/10.1097/BOT.0b013e3181d8893a>.
- Fedorov, A., Beichel, R., Kalpathy-Cramer, J., Finet, J., Fillion-Robin, J.C., Pujol, S., et al., 2012. 3D Slicer as an image computing platform for the Quantitative Imaging Network. *Magn Reson Imaging* 30, 1323–1341. <https://doi.org/10.1016/j.mri.2012.05.001>.
- van der Helm, F.C., 1994a. Analysis of the kinematic and dynamic behavior of the shoulder mechanism. *J Biomech* 27, 527–550.
- van der Helm, F.C., 1994b. A finite element musculoskeletal model of the shoulder mechanism. *J Biomech* 27, 551–569.
- Hulsmans, M.H., van Heijl, M., Houwert, R.M., Burger, B.J., Verleisdonk, E.J.M., Veeger, D.J., et al., 2018. Surgical fixation of midshaft clavicle fractures: A systematic review of biomechanical studies. *Injury* 49, 753–765. <https://doi.org/10.1016/j.injury.2018.02.017>.
- Huttunen, T.T., Launonen, A.P., Berg, H.E., Lepola, V., Fellander-Tsai, L., Mattila, V.M., 2016. Trends in the Incidence of Clavicle Fractures and Surgical Repair in Sweden: 2001–2012. *J Bone Joint Surg Am* 98, 1837–1842. <https://doi.org/10.2106/JBJS.15.01284>.
- Iannolo, M., Werner, F.W., Sutton, L.G., Serell, S.M., VanValkenburg, S.M., 2010. Forces across the middle of the intact clavicle during shoulder motion. *J Shoulder Elbow Surg* 19, 1013–1017. <https://doi.org/10.1016/j.jse.2010.03.016>.
- Klein Breteler, M.D., Spoor, C.W., Van der Helm, F.C., 1999a. Measuring muscle and joint geometry parameters of a shoulder for modeling purposes. *J Biomech* 32, 1191–1197.
- Klein Breteler, M.D., Spoor, C.W., Van der Helm, F.C.T., 1999b. Measuring muscle and joint geometry parameters of a shoulder for modeling purposes. *J Biomech* 32, 1191–1197. [https://doi.org/10.1016/s0021-9290\(99\)00122-0](https://doi.org/10.1016/s0021-9290(99)00122-0).
- Kong, L., Zhang, Y., Shen, Y., 2014. Operative versus nonoperative treatment for displaced midshaft clavicular fractures: a meta-analysis of randomized clinical trials. *Arch Orthop Trauma Surg* 134, 1493–1500. <https://doi.org/10.1007/s00402-014-2077-6>.
- Little, K.J., Riches, P.E., Fazzi, U.G., 2012. Biomechanical analysis of locked and non-locked plate fixation of the clavicle. *Injury* 43, 921–925. <https://doi.org/10.1016/j.injury.2012.02.007>.
- McKee, R.C., Whelan, D.B., Schemitsch, E.H., McKee, M.D., 2012. Operative versus nonoperative care of displaced midshaft clavicular fractures: a meta-analysis of randomized clinical trials. *J Bone Joint Surg Am* 94, 675–684. <https://doi.org/10.2106/JBJS.J.01364>.
- Mellema JJ, Doornberg JN, Guitton TG, Ring D, Science of Variation G. Biomechanical studies: science (f)or common sense? *Injury* 2014;45:2035-2039. [10.1016/j.injury.2014.09.014](https://doi.org/10.1016/j.injury.2014.09.014)
- Nikooyan, A.A., Veeger, H.E., Westerhoff, P., Graichen, F., Bergmann, G., van der Helm,

- F.C., 2010. Validation of the Delft Shoulder and Elbow Model using in-vivo glenohumeral joint contact forces. *J Biomech* 43, 3007–3014. <https://doi.org/10.1016/j.jbiomech.2010.06.015>.
- Nikooyan, A.A., Veeger, H.E., Chadwick, E.K., Praagman, M., Helm, F.C., 2011. Development of a comprehensive musculoskeletal model of the shoulder and elbow. *Med Biol Eng Comput* 49, 1425–1435. <https://doi.org/10.1007/s11517-011-0839-7>.
- Nikooyan, A.A., Veeger, H.E., Westerhoff, P., Bolsterlee, B., Graichen, F., Bergmann, G., et al., 2012. An EMG-driven musculoskeletal model of the shoulder. *Hum Mov Sci* 31, 429–447. <https://doi.org/10.1016/j.humov.2011.08.006>.
- Praagman, M., Chadwick, E.K., van der Helm, F.C., Veeger, H.E., 2006. The relationship between two different mechanical cost functions and muscle oxygen consumption. *J Biomech* 39, 758–765. <https://doi.org/10.1016/j.jbiomech.2004.11.034>.
- Renfree, T., Conrad, B., Wright, T., 2010. Biomechanical comparison of contemporary clavicle fixation devices. *J Hand Surg Am* 35, 639–644. <https://doi.org/10.1016/j.jhsa.2009.12.012>.
- Robertson, G.A., Wood, A.M., Oliver, C.W., 2018. Displaced middle-third clavicle fracture management in sport: still a challenge in 2018. Should you call the surgeon to speed return to play? *Br J Sports Med* 52, 348–349. <https://doi.org/10.1136/bjsports-2016-097349>.
- Robinson, C.M., 1998. Fractures of the clavicle in the adult. *Epidemiology and classification*. *J Bone Joint Surg Br* 80, 476–484.
- Toogood, P., Coughlin, D., Rodriguez, D., Lotz, J., 2014. Feeley B. A biomechanical comparison of superior and anterior positioning of precontoured plates for midshaft clavicle fractures. *Am J Orthop (Belle Mead NJ)* 43, E226–E231.
- Uzer, G., Yildiz, F., Batar, S., Bozdag, E., Kuduz, H., Bilsel, K., 2017. Biomechanical comparison of three different plate configurations for comminuted clavicle midshaft fracture fixation. *J Shoulder Elbow Surg* 26, 2200–2205. <https://doi.org/10.1016/j.jse.2017.06.034>.
- Van der Helm, F.C., Veenbaas, R., 1991. Modelling the mechanical effect of muscles with large attachment sites: application to the shoulder mechanism. *J Biomech* 24, 1151–1163.
- Wu, G., van der Helm, F.C., Veeger, H.E., Makhssous, M., Van Roy, P., Anglin, C., et al., 2005. ISB recommendation on definitions of joint coordinate systems of various joints for the reporting of human joint motion—Part II: shoulder, elbow, wrist and hand. *J Biomech* 38, 981–992.
- Zlowodzki, M., Zelle, B.A., Cole, P.A., Jeray, K., McKee, M.D., 2005. Evidence-Based Orthopaedic Trauma Working G. Treatment of acute midshaft clavicle fractures: systematic review of 2144 fractures: on behalf of the Evidence-Based Orthopaedic Trauma Working Group. *J Orthop Trauma* 19, 504–507.